

Shielding Effectiveness of Three Dimensional Gratings using the Periodic FDTD Technique and CPML Absorbing Boundary Condition

J.Alan Roden, J. Paul Skinner, and Steven L. Johns
The Aerospace Corporation
Chantilly, Va, 20151, USA

Abstract: This paper examines the benefits of grating thickness in regards to enhancing EMI attenuation. Analysis is performed using the FDTD technique using periodic boundary conditions along with new formulations of the CPML absorbing boundary. Furthermore, it is demonstrated that a simple waveguide below cutoff approximation provides accurate results for the normal incident plane wave case.

Keywords: CPML, FDTD, Grating, Shielding Effectiveness (SE), EMI

1. Introduction

Metalized gratings are often used in shielded enclosure designs to allow ventilation or conduits for conductors while attenuating electromagnetic energy. While many designs use waveguide below cutoff principles to insure adequate attenuation, cost many times prohibits such robustness. The focus of this paper is to examine the effectiveness of gratings, grills, or vent arrays as the thickness of these structures are increased.

2. CPML formulation within the Periodic FDTD

Periodic analysis codes are uniquely suited for problems involving large arrays of apertures which are illuminated by plane waves. If one assumes that no near field sources are present, this type of analysis can provide good performance metrics for typical air vent or cable pass-through structures. The solution method in this work is the periodic split-field FDTD (SF-FDTD) as first introduced by Roden, et al [1],[2] and documented later in [3].

Proper implementation of the PML absorbing boundary within the split field implementation periodic FDTD (SF-FDTD) has been documented previously [3]. In that work, the PML update equation was accomplished using a split field approach. A more robust implementation may be accomplished using the recently introduced convolution PML (CPML). The advantage of incorporating the CPML within SF-FDTD is that the additional PML overhead is transparent so far as the implementation of the split field update expressions and significant attenuation of evanescent modes is accomplished. The frequency domain expressions for Ampere's law including CPML are given by

$$\frac{j\omega\epsilon_r}{c_0} \tilde{P}_x + \sigma \tilde{P}_x = \frac{\partial}{\partial y} \tilde{Q}_z - \frac{1}{s_z(\omega)} \frac{\partial}{\partial z} \tilde{Q}_y - j\omega \frac{\sin \theta \sin \phi}{c_0} \tilde{Q}_z \quad (1)$$

$$\frac{j\omega\epsilon_r}{c_0} \tilde{P}_y + \sigma \tilde{P}_y = \frac{1}{s_z(\omega)} \frac{\partial}{\partial z} \tilde{Q}_x - \frac{\partial}{\partial x} \tilde{Q}_z + j\omega \frac{\sin \theta \cos \phi}{c_0} \tilde{Q}_z \quad (2)$$

$$\frac{j\omega\epsilon_r}{c_0} \tilde{P}_z + \sigma \tilde{P}_z = \frac{\partial}{\partial x} \tilde{Q}_y - \frac{\partial}{\partial y} \tilde{Q}_x - j\omega \frac{\sin \theta \cos \phi}{c_0} \tilde{Q}_y + j\omega \frac{\sin \theta \sin \phi}{c_0} \tilde{Q}_x \quad (3)$$

Report Documentation Page				Form Approved OMB No. 0704-0188	
Public reporting burden for the collection of information is estimated to average 1 hour per response, including the time for reviewing instructions, searching existing data sources, gathering and maintaining the data needed, and completing and reviewing the collection of information. Send comments regarding this burden estimate or any other aspect of this collection of information, including suggestions for reducing this burden, to Washington Headquarters Services, Directorate for Information Operations and Reports, 1215 Jefferson Davis Highway, Suite 1204, Arlington VA 22202-4302. Respondents should be aware that notwithstanding any other provision of law, no person shall be subject to a penalty for failing to comply with a collection of information if it does not display a currently valid OMB control number.					
1. REPORT DATE 01 JAN 2005		2. REPORT TYPE N/A		3. DATES COVERED -	
4. TITLE AND SUBTITLE Shielding Effectiveness of Three Dimensional Gratings using the Periodic FDTD Technique and CPML Absorbing Boundary Condition				5a. CONTRACT NUMBER	
				5b. GRANT NUMBER	
				5c. PROGRAM ELEMENT NUMBER	
6. AUTHOR(S)				5d. PROJECT NUMBER	
				5e. TASK NUMBER	
				5f. WORK UNIT NUMBER	
7. PERFORMING ORGANIZATION NAME(S) AND ADDRESS(ES) The Aerospace Corporation Chantilly, Va, 20151, USA				8. PERFORMING ORGANIZATION REPORT NUMBER	
9. SPONSORING/MONITORING AGENCY NAME(S) AND ADDRESS(ES)				10. SPONSOR/MONITOR'S ACRONYM(S)	
				11. SPONSOR/MONITOR'S REPORT NUMBER(S)	
12. DISTRIBUTION/AVAILABILITY STATEMENT Approved for public release, distribution unlimited					
13. SUPPLEMENTARY NOTES See also ADM001846, Applied Computational Electromagnetics Society 2005 Journal, Newsletter, and Conference., The original document contains color images.					
14. ABSTRACT					
15. SUBJECT TERMS					
16. SECURITY CLASSIFICATION OF:			17. LIMITATION OF ABSTRACT UU	18. NUMBER OF PAGES 4	19a. NAME OF RESPONSIBLE PERSON
a. REPORT unclassified	b. ABSTRACT unclassified	c. THIS PAGE unclassified			

where

$$s_i = \frac{1}{\kappa_i + \frac{\sigma_i}{j\omega\epsilon_0 + \alpha}}. \quad (4)$$

and

$$\tilde{P} = \vec{E}\sqrt{\eta_0} \exp(-ik_0 [\sin\theta \cos\phi x + \sin\theta \sin\phi y + \cos\theta z]) \quad (5)$$

$$\tilde{Q} = \vec{H} / \sqrt{\eta_0} \exp(-ik_0 [\sin\theta \cos\phi x + \sin\theta \sin\phi y + \cos\theta z]). \quad (6)$$

In (4), the variable σ_i determines the attenuation rate of propagating waves within the PML, while κ_i, α_i determine the attenuation of evanescent waves within the PML. The basic formulation consists of splitting each of these equations (and their E field counterparts) into two parts and introducing an alternate time grid such that the primary and alternate grids are staggered in time by $\frac{1}{2}$ time steps. For each of the two time grids, the normalized field \tilde{P}_x component update becomes

$$\begin{aligned} \tilde{P}_x^{an+1} = & \frac{1}{\left(\frac{\epsilon_r}{c_0\Delta_t} + \sigma\eta\beta\right)} \left\{ \tilde{P}_x^{an} \left(\frac{\epsilon_r}{c_0\Delta_t} - \sigma\eta\beta \right) - \sigma\eta(1-2\beta) \tilde{P}_x^{an+1/2} \right. \\ & \left. + \frac{\Delta_x}{\Delta_y\Delta_z} \left[\tilde{Q}_{zj}^{n+1/2} - \tilde{Q}_{zj-1}^{n+1/2} - \frac{1}{\kappa} \left(\tilde{Q}_{yk}^{n+1/2} - \tilde{Q}_{yk-1}^{n+1/2} \right) \right] + \frac{\eta\sigma \sin\theta \sin\phi}{2\Delta_z} \left(\tilde{Q}_{z1,j}^{n+1/2} + \tilde{Q}_{z1,j-1}^{n+1/2} \right) - \psi_{xz}^n \right\}. \end{aligned} \quad (7)$$

Similar equations are implemented for the remaining field components and these are valid throughout the entire computational domain. Subsequently, summation variables are introduced and appended to the ‘A’ parts of the split field equations [4] resulting from (1) through (4) and are incremented at each half time step as

$$\tilde{P}_x^{an+1/2} = \tilde{P}_x^{an-1/2} + \frac{1}{c_0\Delta_t\mu_r} \left\{ \frac{\partial}{\partial y} \tilde{Q}_z^n + \frac{1}{\kappa} \frac{\partial}{\partial z} \tilde{Q}_y^n + \psi_{px}^n \right\} \quad (8)$$

$$\psi_{qx}^n = a\psi_{qx}^{n-1/2} + b \frac{\partial}{\partial z} \tilde{Q}_y^n, \quad a_i = e^{-\left(\frac{\sigma_i + \sigma}{\epsilon_0\kappa_i + \epsilon_0}\right)\Delta_t/2}, \quad b_i = \frac{\sigma_i}{\sigma_i\kappa_i + \kappa_i^2\alpha} \left[e^{-\left(\frac{\sigma_i + \sigma}{\epsilon_0\kappa_i + \epsilon_0}\right)\Delta_t/2} - 1 \right]. \quad (9)$$

$$(10)$$

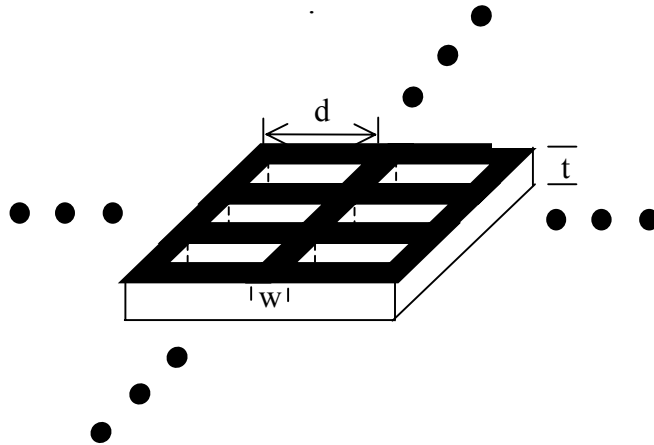


Figure 1 Geometry of this study, infinite array of square apertures.

3. Results

The basic geometry chosen for this study is given in Figure 1. Shown here is a periodic array of square apertures with depth t , which is a variable in the study. For this study, $w=25.0$ mil and $d=400$ mil. A plane wave illuminates the structure from above at an angle θ_i to the surface normal TM polarization. In addition to FDTD simulations, analytic results for the transmission coefficient are computed for the infinitely thin case based on well known formulas. These analytic expressions for transmission and reflection are

$$\tau_{im} = \frac{2Z_s}{2Z_s + Z_0 \cos \theta}, \quad \tau_{ie} = \frac{2Z_s \cos \theta}{2Z_s \cos \theta + Z_0} \quad (11)$$

where θ is the angle of incidence with respect to normal, Z_0 is the impedance of free space, and Z_s is the sheet impedance of the infinitely thin screen which is given by Golden's [5] formula as

$$Z_s^{ie} = \frac{jZ_0 d}{\lambda} \ln \left(\frac{2d}{\pi w} \right), \quad Z_s^{im} = \frac{jZ_0 d \cos \theta}{\lambda} \ln \left(\frac{2d}{\pi w} \right). \quad (12)$$

In (12), d is the center-to-center spacing of the periodic grid, and w is the width of the metal members. Furthermore, wave-guide below cutoff theory is used in order to apply (11) to the general case with thickness. The combination of (11) with this waveguide attenuation (posed for the lowest order mode) provides an easy to use formula for predicting thick surface shielding performance. Figure 2 illustrates the variation of transmission coefficient with varying screen thickness as the depth goes from infinitely thin to $\frac{1}{2}$ inch. Analytic results and FEM results are also presented here and show good agreement. Figure 3 illustrates the effect of varying the incident angle from normal incidence to 60 degrees for TM (to surface) polarization in a principle plane of the lattice.

4. Conclusions

Waveguide below cutoff concepts do provide a good approximation of the effect of adding depth to periodic lattices of apertures in metallic gratings. As a result, one can confidently use such formula for computing the appropriate thickness or depth of such geometries in order to attain a desired EMI attenuation.

The FDTD technique proved quite useful for analyzing these structures and provided quite fast results. The use of the CPML absorbing boundary proved essential to adequately attenuating strong evanescent modes which were present for higher angles of incidence. While the problem studied here contained only metallic materials, the formulation is general and may be applied to a wide array of problems.

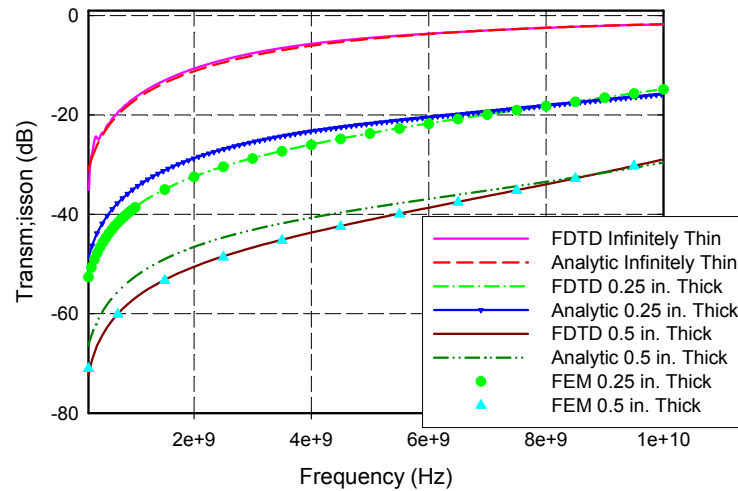


Figure 2 Shielding Effectiveness improvement with varying thickness at zero degrees incident.

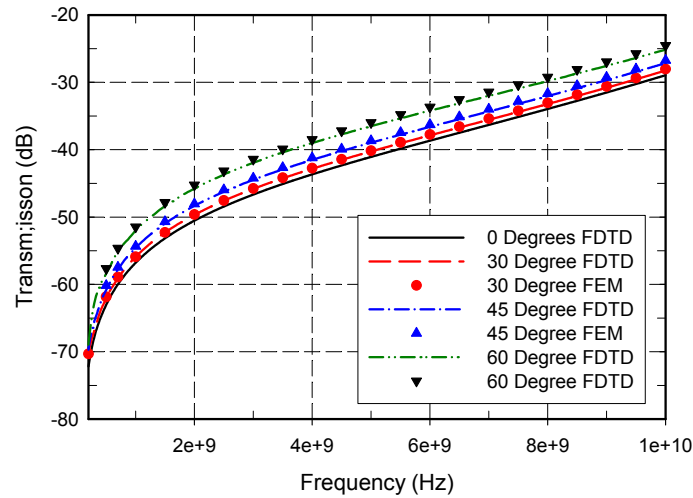


Figure 3 Shielding Effectiveness variation with angle of incidence for 0.5 inch grating.

References

- 1 Roden, J. A., "Electromagnetic Analysis of Complex Structures using the FDTD Technique in General Curvilinear Coordinates", Ph. D. Thesis, *University of Kentucky*, Lexington, KY, 1997.
- 2 Roden, J. A., S. D. Gedney, M. P. Kesler, J. G. Maloney, P. H. Harms, "Time-domain Analysis of periodic structures at Oblique Incidence: Orthogonal and Nonorthogonal FDTD Implementations", *IEEE Trans. Microwave Theory and Techniques*, Vol. 46, 1998, pp 420-427.
- 3 Allan Taflov, "Advances in Computational Electrodynamics, The Finite-Difference Time-domain Method", Artech House, 1998.
- 4 J. A. Roden and S. D. Gedney, "Convolutional PML (CPML): An efficient FDTD implementation of the CFS-PML for arbitrary media", *Microwave and Optical Technology Letters*, Vol 27, 2000.
- 5 K. E. Golden, T. M. Smith, "Simulation of a Thin Plasma Sheath by a Plane of Wires", *IEEE Transactions in Nuclear Science*, Vol NS-11, pp. 225-230, Jan 1964.